Pergamon

Int. J. Heat Mass Transfer. Vol. 40, No. 8, pp. 1937–1945, 1997

0017–9310/97 $17.00+0.00

PII: S0017–9310(96)00240–2

Second-law analysis on a pin-fin array under crossflow

W. W. LIN and D. J. LEE†

Department of Chemical Engineering, National Taiwan University, Taipei, Taiwan 106, Republic of China

(*Received* 10 *January* 1996)

Abstract—Second-law analysis on a pin-fin array under crossflow was conducted, from which the entropy generation rate was evaluated. Increase in the crossflow fluid velocity would enhance the heat transfer rate and hence, reduce the heat transfer irreversibility. Nevertheless, owing to the simultaneous increase in drag force exerting on the fin bodies, the hydrodynamic irreversibility increases as well. An optimal Reynolds number thereby exists over wide operating conditions. Optimal design/operational conditions were searched for on the basis of entropy generation minimized. Comparisons between the staggered and the in-line pin-fin alignments were made in this report. © 1997 Elsevier Science Ltd. All rights reserved.

1. INTRODUCTION

Pin-fin arrays are widely employed to enhance the heat transfer rate in the after-region of a turbine blade or in electronic equipment. In designing a fin array the criterion generally adopted is either to maximize the heat transfer rate under a given fin volume (weight), or to minimize the fin volume under a prescribed heat duty [2–5]. The enhancement of the heat transfer from a fin array had been discussed in refs. [6–8]. Some optimum design methodologies for fin array under natural convection were addressed in refs. [9, 10]. These studies were all based on heat transfer enhancement, or on the first-law analysis.

Recently, second-law analysis has influenced the design methodology of various heat and mass transfer systems [11, 12] to minimize the entropy generation rate, and so to maximize system available work.

In the present work, the second-law analysis on the pin-fin arrays under forced flow condition is considered. Optimal operational/design conditions are evaluated for both the in-line and the staggered fin alignments. The heat transfer configuration under investigation is similar, but not the same as that in ref. [13], in which the heat transfer from the fin surface was totally ignored. In this work, both the heat transfer contributions from the base wall from the fin surface are considered.

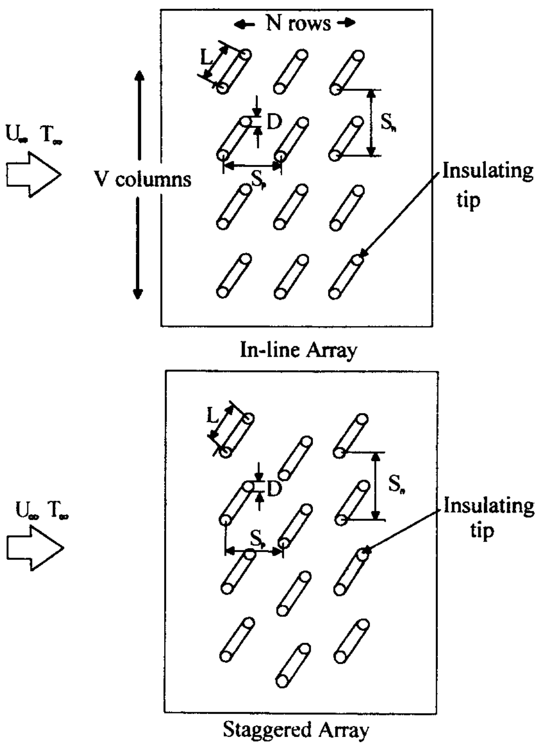

Fig. 1. Schematical drawing of the pin-fin arrays (top) in-line alignment (bottom) staggered alignment.

2. ANALYSIS

The alignment of the fin arrays (N rows $\times$ V columns) are schematically shown in Fig. 1. Assume a small fin Biot number (< 0.1), a constant fin thermal conductivity, a constant heat transfer coefficient and an insulating tip. The relationship between the total base heat flow rate (Q_B) and the temperature difference between fin base and the fluid (θ_B) could be found by solving the heat conduction/convection equation as

$$\theta_\beta = \frac{Q_B}{\frac{\pi}{4}NVkD^2 m \tanh(mL) + h_w(A - \frac{\pi}{4}NVD^2)} \quad (1)$$

† Author to whom correspondence should be addressed.

NOMENCLATURE

A	overall area of wall defined in equation (2b) [m^2]
B	dimensionless group defined in equation (8), dimensionless
D	pin-fin diameter [m]
f	friction factor defined in equation (8), dimensionless
h	heat transfer coefficient [$W\ m^{-2}\ K^{-1}$]
k	thermal conductivity of fin material, [$W\ m^{-1}\ K^{-1}$]
L	pin-fin length [m]
m	pin-fin conduction parameter defined in equation (2a), dimensionless
N	number of rows in a bank, dimensionless
N_s	entropy generation number, defined in equation (6), dimensionless
Nu	Nusselt number, dimensionless
P	pressure [$N\ m^{-2}$]
Pr	Prandtl number, dimensionless
Q_B	total base heat flow rate [W]
Re_D	Reynolds number, DU_{max}/ν
S_{gen}	entropy generation rate [$W\ K^{-1}$]
S_n	pin spacing in spanwise direction [m]
S_p	pin spacing in streamwise direction [m]
T_∞	absolute temperature of free stream [K]
U_{max}	average velocity in the minimum flow area [$m\ s^{-1}$]
U_∞	crossflow approaching velocity [$m\ s^{-1}$]
V	number of columns in a bank, dimensionless
W	slenderness ratio, dimensionless.

Greek symbols

θ_B	base-stream temperature difference [K]
λ	thermal conductivity of fluid [$W\ m^{-1}\ K^{-1}$]
ν	kinematic viscosity of fluid [$m\ s^{-2}$]
ρ	density of fluid [$kg\ m^{-3}$].

where

$$m = \left(\frac{4h}{kD}\right)^{1/2} \tag{2a}$$

$$A = [(N-1)S_p + D][(V-a)S_n + D] \tag{2b}$$

and a is 1 or 1/2 for in-line for staggered fin arrays, respectively. The basic characteristics of the following results would not change for a fin with a non-insulating tip.

Fin effectiveness can be evaluated as the ratio of the base heat flux with and without a fin. The result is:

$$\varepsilon = \left[\frac{\pi}{4}NVkD^2 m \tanh(mL) + h_w\left(A - \frac{\pi}{4}NVD^2\right)\right]/[h_w A]. \tag{3}$$

By assuming a $\theta_B/T_\infty < 0$, the entropy generation rate for a fluid flowing across a submerged body has been stated as [11]:

$$S_{gen} = \frac{Q_B\theta_B}{T_\infty^2} + \frac{\dot{m}\Delta P}{\rho T_\infty} \tag{4}$$

where ΔP is the pressure difference across the body, while

$$\dot{m} = \rho U_{max} L(V-a)(S_n - D). \tag{5}$$

U_{max} is the maximum average fluid velocity occurring at the minimum free area of the fin array.

Substituting equations (1), (2) and (5) into equation (4), with the dimensionless entropy generation number as defined in ref. [11], leads to the following equation for a pin-fin array:

$$Ns = \frac{S_{gen}}{(Q_B^2\, U_{max}/kvT_\infty^2)} = N_{sH} + N_{sF}. \tag{6}$$

N_{sH} is the entropy generation rate owing to heat transfer irreversibility and is equal to:

$$N_{sH} = \left\{\frac{\pi}{2}NV[Nu(\lambda/k)]^{1/2} Re_D \times \tanh[2Nu(\lambda/k)]^{1/2} W] + Nu_w(\lambda/k)Re_D(\lambda.k)Re_D \times \left\{\left[(N-1)\left(\frac{S_p}{S_n}\right)\left(\frac{S_n}{D}\right)+1\right] \times \left[(V-a)\left(\frac{S_n}{D}\right)+1\right] - \frac{\pi}{4}NV\right\}\right\}^{-1}. \tag{7a}$$

N_{sF} is due to the fluid flow irreversibility and is as follows:

$$N_{sF} = \frac{1}{2}BfN(V-a)\left(\frac{S_n}{D}-1\right)Re_D W. \tag{7b}$$

The dimensionless groups appearing in equations (7a) and (7b) are defined as follows:

$$Nu = \frac{hD}{\lambda} \quad Nu_w = \frac{h_w D}{\lambda}$$

$$Re_D = \frac{U_{max}D}{\nu} \quad Re_L = \frac{U_{max}L}{\nu} \tag{8}$$

Table 1. Values of C and n in equation (9) [14]

Re_D range		Staggered arrays C	n	In-line arrays C	n
10–100		0.8	0.4	0.9	0.4
100–1000		0.71	0.5	0.52	0.5
$1000–2\times10^5$	$(S_n/S_p) < 2$	$0.35(S_p/S_n)^{-0.2}$	0.6	0.27	0.63
	$(S_n/S_p) > 2$	0.4	0.6		
$2\times10^5–10^6$		$0.031(S_p/S_n)^{-0.2}$	0.88	0.03	0.8

$$f = \frac{\Delta P}{\frac{1}{2}\rho U_{max}^2 N} \quad B = \frac{\rho v^3 k T_\infty}{Q_B^2} \quad W = \frac{L}{D}.$$

The Nusselt number (Nu) and the friction factor (f) can be evaluated from the results for a bank of tubes in a crossflow [14, 15]. The Nusselt number for $N \geqslant 20$ can be found as

$$Nu = CRe_D^n Pr^{0.36}. \tag{9}$$

Values of C and n are listed in Table 1 [14]. The heat transfer coefficient of wall was assumed as that of the fin surface (i.e. $Nu_w = Nu$) for the sake of simplicity [9]. On the other hand, the following correlations can be employed for friction factor [14, 15]:

$$f = \left[0.176 + \frac{0.32\left(\frac{S_p}{S_n}\right)\left(\frac{S_n}{D}\right)}{\left(\frac{S_n}{D}-1\right)^{0.43+1.13(D/S_n)(S_n/S_p)}}\right] \times Re_D^{-0.15} \quad \text{for in-line arrays} \tag{10a}$$

or

$$f = \left[1.0 + \frac{0.47}{\left(\frac{S_n}{D}-1\right)^{1.08}}\right] Re_D^{-0.16} \quad \text{for staggered arrays.} \tag{10b}$$

The entropy generation number, N, is thereby a function of nine dimensionless groups: two for the fin geometry (Re_D, W), four for the array parameter (S_p/S_n, S_n/D, N, V), and two for the working fluid and the heat duty (M $(=(k/\lambda)^{1/2}/Pr^{1/6})$, B).

For a fixed fin array and a given heat duty, the last eight parameters were fixed. The minimum of N_s with respect to Re_D can thereby be evaluated by solving $\partial N_S/\partial Re_D = 0$ graphically, while the corresponding optimal $Re_{D,opt}$, can be subsequently obtained.

3. RESULTS AND DISCUSSION

3.1. *Optimal Reynolds number*

Figure 2 shows an example of the N_s vs Reynolds number plot for the in-line and the staggered alignments at fixed fin geometry. N_{sH} (N_{SF}) decreases (increases) with an increase in Re_D for both the in-line (bold curves) and the staggered (dashed curves) arrays. An optimal Reynolds number results away from which the entropy generation rate would increase. The optimal Re_D values read 2068 for the in-line or 1974 for the staggered alignment. The corresponding entropy generation numbers are, respectively, 9.06×10^{-5} and 9.36×10^{-5}, indicating a better 'best' overall performance for the in-line alignment can be achieved than that for the staggered alignment in this specific example. It is also noted that in the range where $Re_D < Re_{D,opt}$, the in-line array would generate more entropy than does the staggered array. That is, the latter would be the better choice if the flow condition must be located in this region. Apparently, the situation would reverse when $Re_D > Re_{D,opt}$.

In the following discussions, we will focus on the effects of geometrical factors on the second law performance.

3.2. *Slenderness ratio*

The effects of slenderness ratio W ($= L/D$) on the entropy generation rate are shown in Fig. 3. $Re_{D,opt}$ increases with the decreasing slenderness ratio. However, the corresponding entropy generation number decreases only slightly. This result is similar to that for a single pin-fin [11]. No slenderness ratio, W, for the fin array needs to be strongly recommended by the second-law analysis, if the crossflow condition can be specified at $Re_D = Re_{D,opt}$.

The corresponding heat transfer characteristics from the first-law analysis are shown in Fig. 4. Note that only a mild decrease in effectiveness results as the Reynolds number increases. This is raised naturally from the simultaneous increase in both the heat fluxes from the fin surface and from the bare base if the fin does not exist at an increasing crossflow velocity. Owing to the slowly decreasing fin effectiveness obtained in the first-law analysis, a small fin Reynolds number is recommended (although not strongly), for example, 1000 if based on the data in Fig. 4.

The optimal Reynolds numbers from Fig. 3 are also shown in Fig. 4 for comparison. Notably, when compared with the first-law analysis, second-law analysis has recommended a definitely best fin Reynolds number. Although when compared with the case

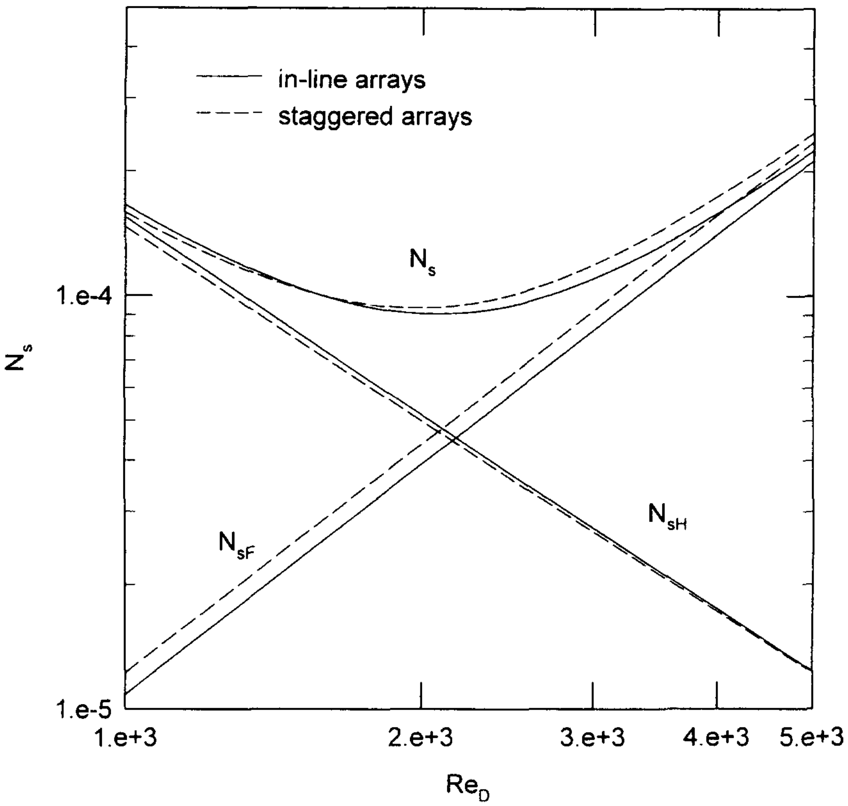

Fig. 2. Entropy generation number vs Re_D, N_{sF} and N_{sH} are the contribution by hydrodynamic and heat transfer irreversibilities, respectively. Solid curves are for in-line array, while dashed curves are for staggered array. $M = 100$, $B = 10^{-13}$, $W = 5$, $S_p/S_n = 1$, $S_n = 1$, $S_n/D = 1.25$, $N = 20$, $V = 10$.

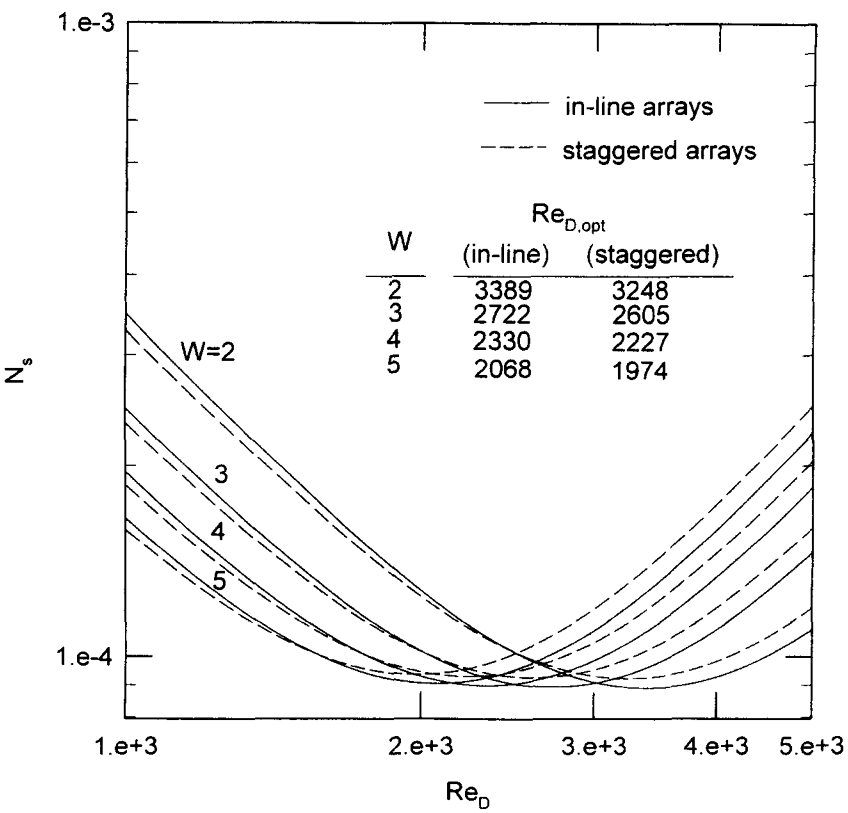

Fig. 3. Entropy generation number vs Re_D under various W. Solid curves are for in-line array, while dashed curves are for staggered array. $M = 100$, $B = 10^{-13}$, $S_p/S_n = 1$, $S_n/D = 1.25$, $N = 20$, $V = 10$.

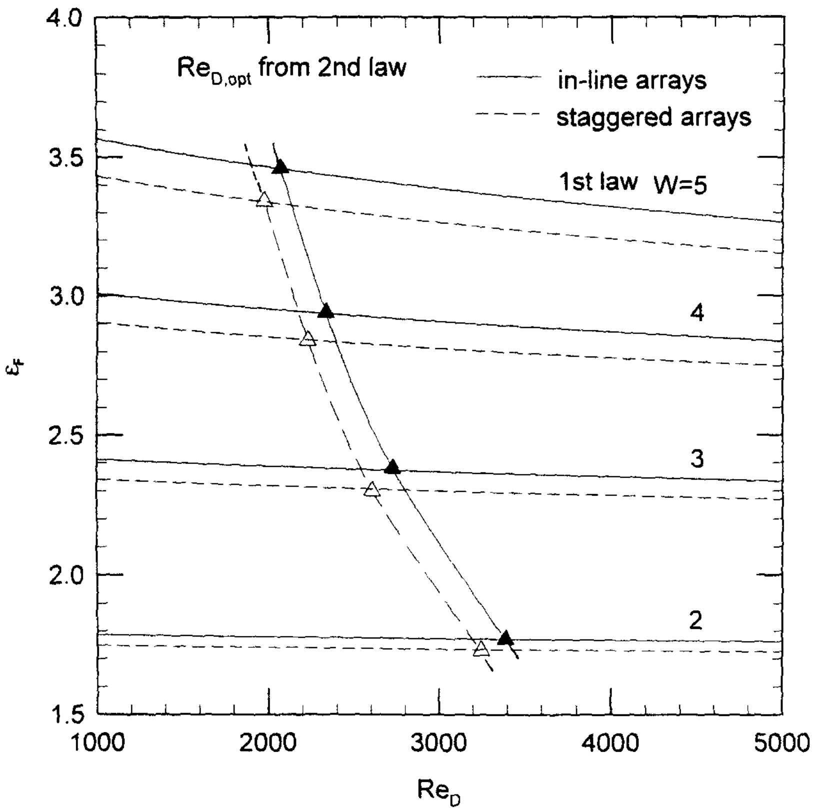

Fig. 4. Fin effectiveness vs Re_D under various W. Solid curves are for in-line array, while dashed curves are for staggered array. The solid symbols are the optimal Reynolds numbers obtained from Fig. 3. $M = 100$, $B = 10^{-13}$, $S_p/S_n = 1$, $S_n/D = 1.25$, $N = 20$, $V = 10$.

$Re_D = 1000$, the fin effectiveness under $Re_{D,opt}$ is somewhat less, as indicated in Fig. 4, however, the overall entropy generation number would be up to 1.7–4 times $N_{s,min}$ if $Re_D = 1000$. Notably, the so-called 'optimal' fin design based on the second-law analysis would usually be not as 'bad' design in view of the first-law analysis (the fin effectiveness is still high).

If based on the heat transfer argumentation, a large slenderness ratio is suggested by the first-law analysis. This conclusion is supported by the second-law analysis if $Re_D < Re_{D,opt}$. Nevertheless, in the range of $Re_D > Re_{D,opt}$, an opposite conclusion would be obtained.

3.3. *Fin spacing*

Figure 5 depicts the N_s vs Re_D plot with $W = 5$ and $S_p/S_n = 1$ and S_n/D as a parameter. For the staggered alignment, the optimal Reynolds number, $Re_{D,opt}$, increases with decreasing S_n/D. On the other hand, for the in-line alignment, the $Re_{D,opt}$ exhibits a maximum as S_n/S_D increases.

The corresponding minimum entropy generation number is plotted against S_n/D in Fig. 6 with the heat dissipation number B as a parameter. Two things are noticeable: firstly, $N_{s,min}$ would increase monotonously with the increase in S_n/D for the staggered alignment; there is a minimum of $N_{s,min}$ for the in-line alignment. Secondly the minimum entropy generation rate for the staggered alignment would be higher than that for the in-line alignment when S_n/D is larger than approximately 1.22. Below this critical value, the staggered alignment would be a better choice based on the second-law analysis. Interpretations will be given in the last sections.

Figure 7 shows the N_s vs Re_D plot under various S_p/S_n values with fixed W and S_n/D. For the in-line alignment, the optimal Reynolds number increases with decreasing S_p/S_n. The corresponding entropy generation number follows a reversed trend. For the staggered-aligned arrays, the N_s vs Re_D curves almost coincide with each other. That is, the entropy generation number is almost independent of the S_p/S_n value.

The corresponding $N_{s,min}$ values are demonstrated in Fig. 8 with the heat dissipation number B as a parameter. Clearly the minimum entropy generation number decreases with increasing S_p/S_n for the staggered alignments. An opposite trend is observed for the in-line alignment. Like that demonstrated in Fig. 6, there also exists a critical S_p/S_n for each B value dividing the region in which the staggered or the in-line alignment is preferred. Interpretations for the S_p/S_n effects will also be given later.

A fin array design with a lesser minimum entropy generation rate would be economically more preferable. With a fixed heat dissipation number and slen-

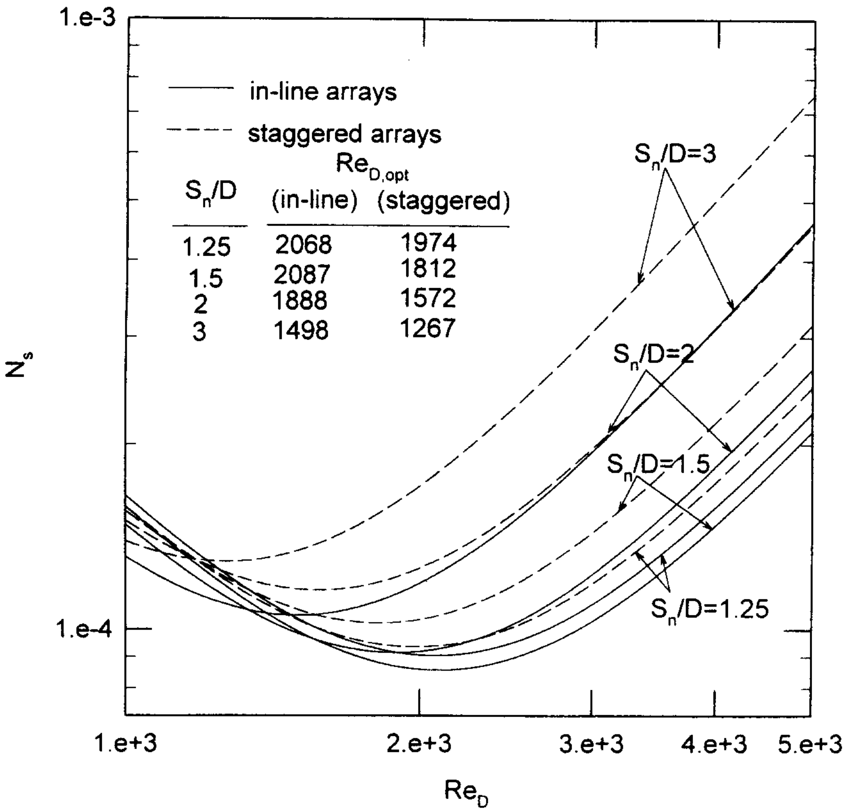

Fig. 5. Entropy generation number vs Re_D under various S_n/D. Solid curves are for in-line array, while dashed curves are for staggered array. $M = 100$, $B = 10^{-13}$, $S_p/S_n = 1$, $W = 5$, $N = 20$, $V = 10$.

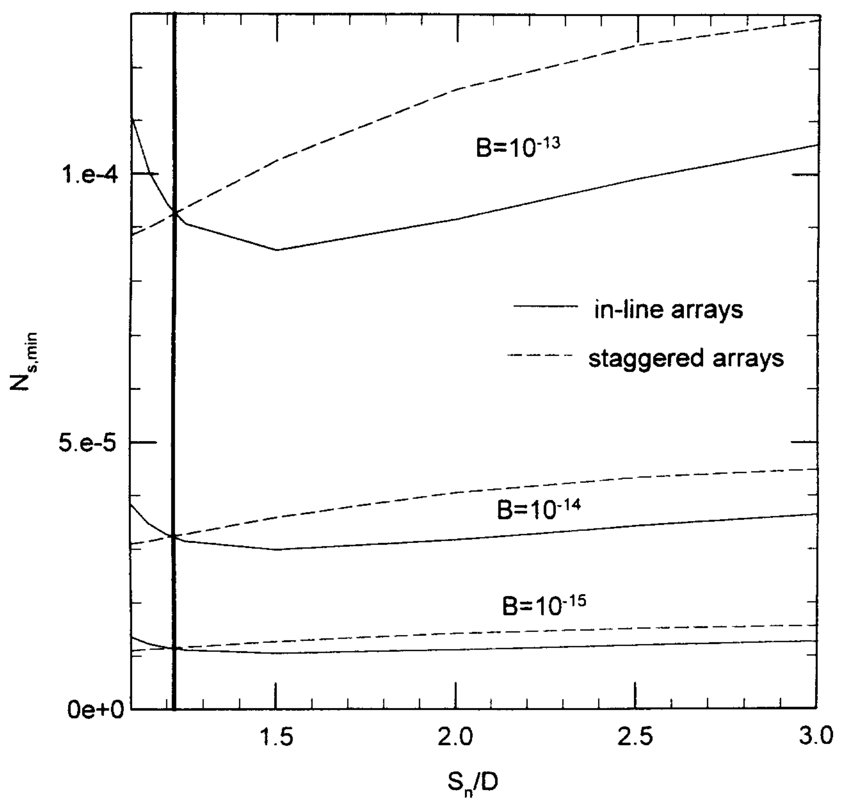

Fig. 6. Minimum entropy generation number vs S_n/D under various heat dissipation number B. Solid curves are for in-line array, while dashed curves are for staggered array. $M = 100$, $S_p/S_n = 1$, $W = 5$, $N = 20$, $V = 10$.

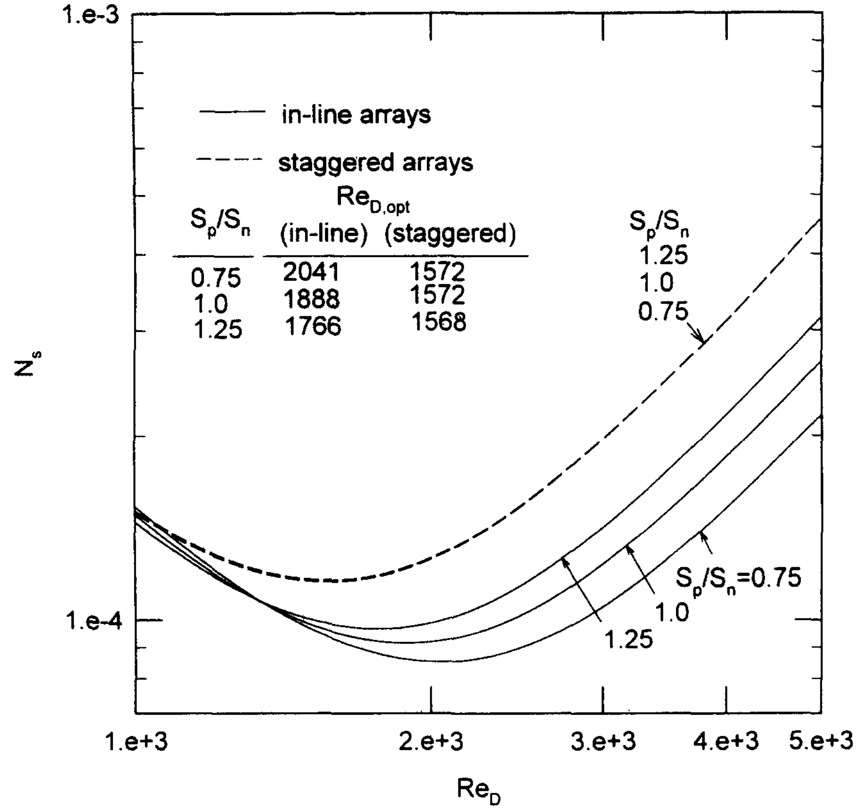

Fig. 7. Entropy generation number vs Re_D under various S_p/S_n. Solid curves are for in-line array, while dashed curves are for staggered array. $M = 100$, $B = 10^{-13}$, $W = 5$, $S_n/D = 2$, $N = 20$, $V = 10$.

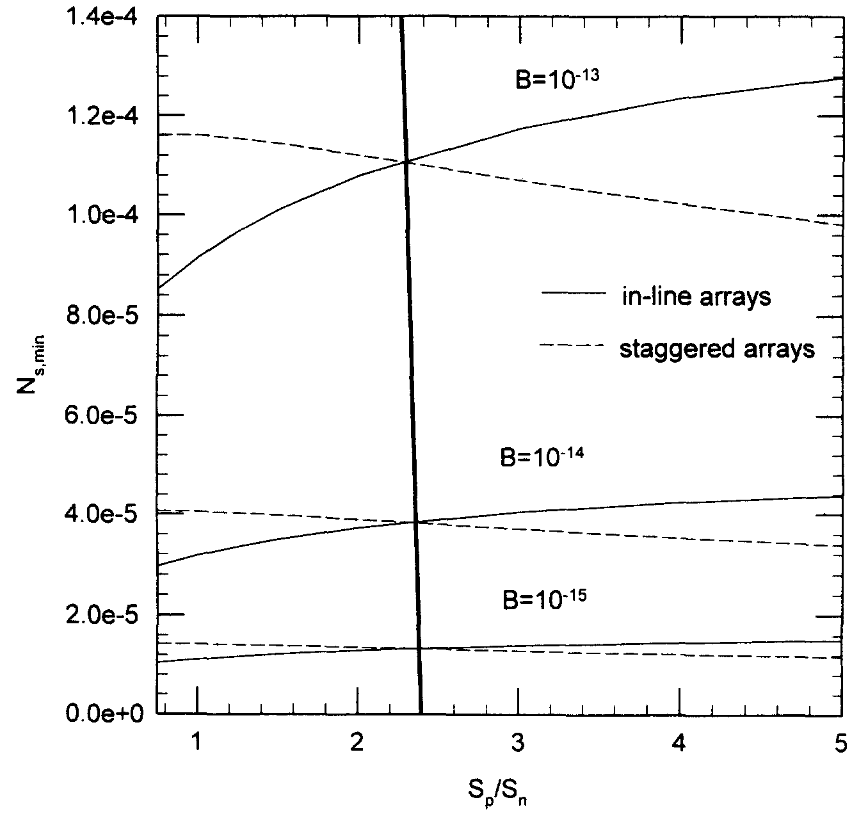

Fig. 8. Minimum entropy generation number vs S_p/S_n under various heat dissipation number B. Solid curves are for in-line array, while dashed curves are for staggered array. $M = 100$, $W = 5$, $S_n/D = 2$, $N = 20$, $V = 10$.

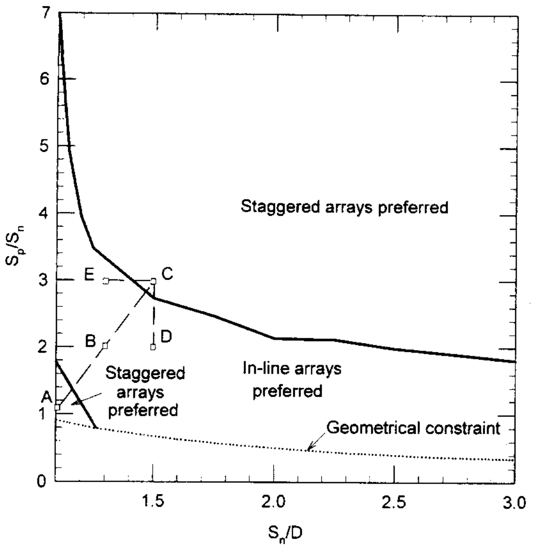

Fig. 9. The map for the region within which the in-line or staggered alignment is preferred. $M = 100$, $B = 10^{-13}$, $W = 5$, $N = 20$, $V = 10$.

derness ratio, the condition under which the ratio between the minimum entropy generation number for staggered and in-line alignments is unity, can be calculated. Figure 9 provides a calculation example, for which the bold curves demonstrate the condition and the ratio of minimum entropy generation numbers equals unity. The dot curve near the abscissa indicates the naturally geometrical restrictions.

Notably from Fig. 9, the staggered array would be preferred in the region of larger S_n/D and S_p/S_n, while the in-line alignment becomes the better choice in the intermediate region. There exists a small region near the ordinate where the staggered alignment would be better again.

More insights can be obtained on the basis of the corresponding f, Nu, $N_{sF,min}$ and $N_{sH,min}$ values under $Re_D = Re_{D,opt}$ (listed in Table 2) for points A–E shown in Fig. 9. For example, the comparisons between points E and C, or points B and D, give the effects of S_n/D under some S_p/S_n; while those between points B and E, or points D and C, give the effects of S_p/S_n under a fixed S_n/D value.

At point C in Fig. 9, both the Nu and the f for the in-line array are higher than those for the staggered array. The relatively higher f and Nu values for the in-line array thereby prefer a somewhat lower optimal Reynolds number. The higher f value gives a larger $N_{sF,min}$ for the in-line array. Although the Nu is also larger, the corresponding $N_{sH,min}$ for in-line array would still be greater owing to the relatively smaller Reynolds number (equation (7a)). This gives out a higher $N_{s,min}$ for in-line array and makes the staggered array a more preferable choice.

Moving from point C to point E (decreasing S_n/D values with a fixed S_p/S_n), owing to the reduction in fluid passage area, both the f and Nu increase accordingly. The corresponding $N_{sH,min}$ and $N_{sF,min}$ are both reduced according to the higher heat transfer rate. Since the relative magnitude of increase in Nu (f) is larger (less) for the in-line array, the rate of reduction in $N_{sF,min}$ and $N_{sH,min}$ are all higher than the staggered array, which in turns gives out a lower $N_{s,min}$ for the in-line array and makes it a preferable choice. This can explain the critical S_n/D value as observed in Fig. 6.

Moving from point C to point D (decreasing S_p/S_n values at fixed S_n/D), the Nusselt number increases for both arrays as for the case of decreasing S_n/D value. The friction factor, on the contrary, reduces rather than increases (although the dependence observed for the staggered array is very weak). This is possibly due to the shrinkage of the wake flow when the distance between the rows are close. For the in-line array, the corresponding low friction factor and higher Nu result in a higher $Re_{D,opt}$. This would give out smaller $N_{sH,min}$ and $N_{sF,min}$ values when moving from point C to D. The trend for the staggered array is opposite. The net effect is to make the in-line array a better choice, which gives an explanation for the existence of the critical S_n/D as observed in Fig. 8.

Comparison between points C, B and A in Fig. 9, reflects a combined effect of reduction in S_n/S_p and S_n/D values. A similar trend can be observed as dis-

Table 2. Corresponding entropy generation numbers, Nusselt number and friction factor under $Re_{D,opt}$ for points A–E shown in Fig. 9

Point	$Re_{D,opt}$	$N_{s,min}$	$N_{sH,min}$	$N_{sF,min}$	$Nu(\lambda/k)$	f
			In-line arrays			
A	1906	1.045×10^{-4}	5.646×10^{-5}	4.805×10^{-5}	3.147×10^{-3}	2.939
B	1943	8.999×10^{-5}	4.855×10^{-5}	4.145×10^{-5}	3.185×10^{-3}	8.133×10^{-1}
C	1607	1.031×10^{-4}	5.543×10^{-5}	4.771×10^{-5}	2.826×10^{-3}	8.211×10^{-1}
D	1804	9.561×10^{-5}	5.149×10^{-5}	4.412×10^{-5}	3.039×10^{-3}	6.025×10^{-1}
E	1779	9.475×10^{-5}	5.102×10^{-5}	4.373×10^{-5}	3.013×10^{-3}	1.023
			Staggered arrays			
A	2085	8.889×10^{-5}	4.831×10^{-5}	4.058×10^{-5}	3.367×10^{-3}	1.965
B	1975	9.680×10^{-5}	5.245×10^{-5}	4.435×10^{-5}	2.876×10^{-3}	8.126×10^{-1}
C	1798	1.005×10^{-4}	5.430×10^{-5}	4.624×10^{-5}	2.521×10^{-3}	6.023×10^{-1}
D	1816	1.026×10^{-4}	5.548×10^{-5}	4.710×10^{-5}	2.750×10^{-3}	6.013×10^{-1}
E	1950	9.592×10^{-5}	5.186×10^{-5}	4.406×10^{-5}	2.647×10^{-3}	8.131×10^{-1}

cussed above. Clearly, the preferred array changes from staggered to in-line alignment when moving from point C to point B. However, since the friction factor increases significantly when the rows are very close [16] (point A), the values $N_{s,min}$ for both arrays increase accordingly. The magnitude of increase in f for in-line array is larger than that for staggered array. This again makes the staggered array a better choice.

4. CONCLUSIONS

Second-law analysis on a pin-fin array under crossflow was conducted, from which the entropy generation rate was evaluated. Increase in the crossflow fluid velocity would enhance the heat transfer rate and reduce the heat transfer irreversibility. Owing to the simultaneous increase in drag force exerting on the fin bodies, the hydrodynamic irreversibility increases as well. An optimal Reynolds number thereby exists over wide operating conditions. Optimal design/operational conditions were searched for on the basis of entropy generation minimization. Comparisons between the staggered and the in-line pin-fin alignments were made in this report.

REFERENCES

1. Kern, D. Q. and Kraus, A. D., *Extended Surface Heat Transfer*. McGraw-Hill, New York, 1972.
2. Yeh, R. H., Optimum designs of longitudinal fins. *The Canadian Journal of Chemical Engineering*, 1995, **73,** 181–189.
3. Guceri, S. and Maday, C. J., A least weight circular cooling fin. *Journal of Engineering in Industry*, 1975, **97,** 1190–1193.
4. Razelos, P. and Imre, K., Minimum mass convective fins with variable heat transfer coefficients. *Journal of the Franklin Institute*, 1983, **315,** 269–282.
5. Razani, A. and Zohoor, H. Optimum dimensions of convective-radiative spines using a temperature correlated profile. *Journal of the Franklin Institute*, 1991, **328,** 471–486.
6. Goldstein, R. J., Jabbari, M. Y. and Chen, S. B., Convective mass transfer and pressure loss characteristics of staggered short pin-fin arrays. *International Journal of Heat and Mass Transfer*, 1994, **37,** 149–160.
7. Jubran, B. A., Hamdan, M. A. and Abdualh, R. M., Enhanced heat transfer, missing pin, and optimization for cylindrical pin fin arrays. *ASME Journal of Heat Transfer*, 1993, **115,** 576–583.
8. Chyu, M. K., Heat transfer and pressure drop for short pin-fin arrays with pin-endwall fillet. *ASME Journal of Heat Transfer*, 1990, **112,** 926–932.
9. Yeh, R. H. and Chang, M., Optimum longitudinal convective fin arrays. *International Communication in Heat and Mass Transfer*, 1995, **22,** 445–460.
10. Jones, C. D. and Smith, L. F., Optimum arrangement of rectangular fins on horizontal surfaces for free-convection heat transfer. *ASME Journal of Heat Transfer*, 1970, **92,** 6–10.
11. Bejan, A., *Entropy Generation through Heat and Fluid Flow*. Wiley, New York, 1982.
12. Lee, D. J. and Lin, W. W., Second-law analysis on a fractal-like fin under crossflow, *AIChE Journal*, 1995, **41,** 2314–2317.
13. Schenone, C., Tagliafico, L. and Tanda, G., Second law performance analysis for offset strip-fin heat exchangers. *Heat Transfer Engineering*, 1991, **12,** 19–27.
14. Zukauskas, A. Ulinskas, R., Efficiency parameters for heat transfer in tube banks. *Heat Transfer Engineering*, 1985, **6,** 19–25.
15. Chapman, A. J., *Fundamentals of Heat Transfer*, Macmillan, New York, 1987.
16. Grimison, E. D., Correlation and utilization of new data on flow resistance and heat transfer for cross flow of gases over tube bank. *Transactions of the A.S.M.E.*, 1937, **59,** 583–594.